

# SMSP: A Plug-and-Play Strategy of Multi-Scale Perception for MLLMs to Perceive Visual Illusions

Jinzhe Tu  
tujz23@mails.tsinghua.edu.cn  
The Conversational AI (CoAI) group,  
DCST, Tsinghua University  
China

Ruilei Guo  
Tsinghua University  
China

Zihan Guo  
Tsinghua University  
China

Junxiao Yang  
The Conversational AI (CoAI) group,  
DCST, Tsinghua University  
China

Shiyao Cui  
The Conversational AI (CoAI) group,  
DCST, Tsinghua University  
China

Minlie Huang\*  
aih Huang@tsinghua.edu.cn  
The Conversational AI (CoAI) group,  
DCST, Tsinghua University  
China

## Abstract

Recent works have shown that Multimodal Large Language Models (MLLMs) are highly vulnerable to hidden-pattern visual illusions, where the hidden content is imperceptible to models but obvious to humans. This deficiency highlights a perceptual misalignment between current MLLMs and humans, and also introduces potential safety concerns. To systematically investigate this failure, we introduce IlluChar, a comprehensive and challenging illusion dataset, and uncover a key underlying mechanism for the models' failure: high-frequency attention bias, where the models are easily distracted by high-frequency background textures in illusion images, causing them to overlook hidden patterns. To address the issue, we propose the Strategy of Multi-Scale Perception (SMSP), a plug-and-play framework that aligns with human visual perceptual strategies. By suppressing distracting high-frequency backgrounds, SMSP generates images closer to human perception. Our experiments demonstrate that SMSP significantly improves the performance of all evaluated MLLMs on illusion images, for instance, increasing the accuracy of Qwen3-VL-8B-Instruct from 13.0% to 84.0%. Our work provides novel insights into MLLMs' visual perception, and offers a practical and robust solution to enhance it. Our code is publicly available at <https://github.com/Tujz2023/SMSP>.

## CCS Concepts

• **Computing methodologies** → **Image processing**; *Object recognition*; Image representations.

## Keywords

Multimodal Large Language Models, Visual Illusions, Visual Perception, Robustness

## 1 Introduction

Recent advances have endowed Multimodal Large Language Models (MLLMs) [2, 4, 9, 15, 27] with remarkable visual understanding capabilities [7, 8, 29]. However, recent works [3, 22, 25] reveal that MLLMs remain highly vulnerable to a type of "hidden-pattern visual illusions", images that embed some patterns within a specific background, and the patterns are only visible under altered visual

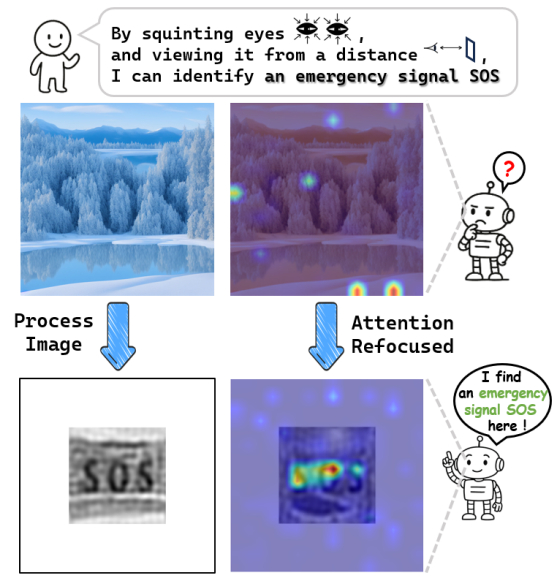


**Figure 1: Top: An illusion image with an emergency signal. The model's attention is dispersed by the background and fails to detect it, while humans can identify it by adjusting their perception. Bottom: After processing the image to simulate such perceptual adjustments, the model can focus on the signal and successfully recognize it.**

focus or viewing conditions. The MLLM's vulnerability to these illusions not only challenges the robustness of their fundamental visual capability [3], but also introduces significant security imperatives, as such illusions can be weaponized to circumvent automated moderation and camouflage malicious content [22].

Existing works [10, 25] mainly focused on embedding simple patterns, such as animals or clothes, into illusion images. However, they lack sufficient exploration of concealing characters, including digits, English letters, and Chinese characters, which are widely used in illusion images on social media. Unlike prior patterns, these characters require more fine-grained recognition due to their more subtle structural details (e.g., distinguishing '6' from '8'), making

\*Corresponding Author

them a great challenge in visual illusions. Our preliminary experiments (detailed in Appendix A) support this observation: Qwen3-VL-8B-Instruct[4], for instance, achieves only 4.8% accuracy on character-based illusions, lower than those with animals (34.0%) or clothes (8.5%) patterns.

Given the challenge of the character-based illusions, we introduce *IlluChar*, an illusion dataset with commonly-used characters as hidden patterns. Unlike prior datasets [22, 25] which mainly embed a single large pattern into AI-generated backgrounds, *IlluChar* embeds characters of more diverse sizes into more background types, making it a more comprehensive and challenging benchmark. Our experiments show that even the most advanced MLLMs suffer an accuracy drop of over 65% on illusion images compared to original clean character images, revealing their high vulnerability in perceiving these illusions.

Given this poor performance, we investigate the failure of MLLMs from two aspects: (1) **the special visual features of illusion images** and (2) **how these features affect the model’s visual capability**. We find that the distracting backgrounds in the illusions introduce strong high-frequency components, which diverts the model’s attention away from the hidden content. We summarize this mechanism as *high-frequency attention bias*. As shown in Figure 1, the model allocates more attention to the background, leading to a recognition failure. In contrast, humans can easily identify the hidden content by adjusting their perception.

Based on the finding, we propose the *Strategy of Multi-Scale Perception (SMSP)*, a human-aligned and plug-and-play framework designed to help models perceive illusions. SMSP first includes a Perception Module that processes the illusion image into a clearer one, thereby guiding the model to reallocate its attention. This process aligns with how humans adjust their perception to obtain more recognizable images. As shown in Figure 1, after applying the Perception Module, the image becomes clearer and the model can focus on the hidden characters. Moreover, as humans can dynamically adapt their perception to illusions with hidden patterns of varying scales, SMSP further employs a Multi-Scale Strategy to simulate this effect, not only enabling the model to handle the scale diversity of the hidden characters, but also preserving its original capability on standard out-of-distribution (OOD) tasks.

Our experiments show that SMSP consistently improves the performance of all evaluated MLLMs on illusion images. For example, it boosts the accuracy of Qwen3-VL-8B-Instruct from 13.0% to 84.0%. The improvements remain consistent across different background types and hidden character scales, demonstrating its effectiveness. Meanwhile, further experiments show that SMSP preserves model’s original performance on OOD tasks, indicating its compatibility.

Beyond the illusion task, our findings suggest that part of the MLLM’s vulnerability may stem from a perceptual misalignment between the model and humans, rather than its insufficient knowledge or model capacity. The effectiveness of SMSP further demonstrates that such misalignment can be mitigated through perception-level adjustments prior to inference, without retraining or modifying model parameters.

Our main contributions are as follows:

- We construct *IlluChar*, a comprehensive and challenging visual illusion dataset that verifies MLLM’s vulnerability on illusion images.

- We identify and characterize the high-frequency attention bias as a key underlying mechanism for MLLM’s failure on visual illusions.
- We propose SMSP, a human-aligned and plug-and-play strategy that effectively improves model’s performance on illusion images with all considered background types and hidden pattern scales.

## 2 Related Work

### 2.1 Visual Illusions

Many studies have investigated various types of visual illusions. For example, several studies focus on classical cognitive illusions [13, 14, 20, 21, 33, 34], such as color and size perception distortions. Other research also explore real scene illusions [26], overlay-style illusions [5], and images with geometric transformations [12].

However, only a limited number of studies investigate illusion images containing hidden patterns, which can be revealed through simple perceptual adjustments. Existing works [10, 22, 25] mainly focus on AI-generated illusions, embedding patterns such as animals and even malicious content into realistic scenes. Meanwhile, another study [11] also investigates generating non-AI-generated illusions, utilizing noisy textures to hide the patterns. Compared to prior studies, our dataset embeds a more challenging pattern type—character—and introduces richer variations in both background construction and hidden characters scales, better simulating the complexity of real-world illusion scenarios.

### 2.2 Analysis and Mitigation of Hidden-Pattern Visual Illusions

Existing research provides limited investigation into the underlying causes of MLLM’s failure on the illusion task, as well as mitigation strategies. Some studies [3, 33] suggest that MLLM’s failure is related to their limitations in visual perception, while another study [22] analyzes factors such as image encoding and attention distribution. Several intuitive mitigation methods [22, 25] have also been explored, including applying Gaussian blur, grid repetition, and histogram-based image transformations. Based on these works, we further conduct a more comprehensive analysis into the underlying mechanism of MLLM’s failure, and propose a plug-and-play strategy that aligns with humans’ perceptual strategies.

Categories	Large	Medium	Small
Origin			
Noise			
Semantic			

Figure 2: Examples across different categories in *IlluChar*.

**Table 1: Accuracies (%) of six MLLMs and human participants on IlluChar.**

Models	Origin				Noise				Semantic			
	Large	Medium	Small	Avg.	Large	Medium	Small	Avg. ( $\Delta \downarrow$ )	Large	Medium	Small	Avg. ( $\Delta \downarrow$ )
Qwen3-VL-8B	87.1	99.3	97.1	93.2	0.6	11.4	48.7	16.7 (-76.5)	2.4	6.4	6.7	3.8 (-89.4)
GLM-4.5V	93.1	97.1	97.1	95.3	1.3	26.3	75.7	28.5 (-66.8)	3.6	6.0	13.3	4.9 (-90.4)
Qwen3-VL-235B-A22B	95.3	100.0	99.3	97.7	0.9	16.4	55.4	20.0 (-77.7)	2.7	7.8	6.7	4.4 (-93.3)
GPT-5.2	77.2	99.3	98.6	89.1	3.1	2.9	26.0	9.3 (-79.8)	4.0	1.4	4.0	3.3 (-85.8)
Gemini-2.5-Pro	91.4	98.6	97.1	94.9	1.7	17.1	74.4	25.8 (-69.1)	4.7	4.6	12.0	5.2 (-89.7)
Claude-Sonnet-4.5	75.0	97.9	97.9	87.5	1.4	1.7	0.3	1.2 (-86.3)	3.0	3.2	9.3	3.5 (-84.0)
<b>Human</b>	-	-	-	-	<b>98.9</b>	<b>100.0</b>	<b>100.0</b>	<b>99.5</b>	<b>98.7</b>	<b>99.3</b>	<b>100.0</b>	<b>99.0</b>

### 3 IlluChar: A Character-Based Illusion Dataset

#### 3.1 Dataset Overview

We introduce **IlluChar**, a comprehensive and challenging character-based illusion dataset for MLLMs. Each image ( $1000 \times 1000$  resolution) embeds specific characters within a generated background.

For hidden patterns, we select commonly-used characters, including 10 digits, 52 uppercase and lowercase English letters, and 170 high-usage Chinese characters, which are prevalent in illusion images on social media and contain subtle structural details. Moreover, to simulate real-world settings where the hidden patterns may appear at varying spatial scales, our dataset includes characters of different sizes. Based on their scales, we categorize all the images into **large, medium, and small** scale groups.

For backgrounds, we consider two categories: **Semantic Backgrounds** and **Noise Backgrounds**, which are both proved effective to generate visual illusions [11, 25]. Semantic Backgrounds refer to AI-generated realistic scenes, while Noise Backgrounds are non-AI-generated pure noise textures such as gratings or Gaussian noise.

Unlike prior datasets [22, 25], IlluChar mainly focuses on characters, and incorporates more varying pattern scales and background types, making it a more comprehensive and challenging benchmark for MLLMs. We provide some examples in Figure 2.

#### 3.2 Dataset Construction

We first render the hidden characters of each illusion image onto a clean white background to obtain the corresponding original image. To generate characters of different scales, we place character strings of different lengths within images of the same resolution, thereby producing different character sizes.

We then construct illusion images with two types of backgrounds. For the Semantic Background illusions, we employ Stable Diffusion [24] with ControlNet [32] to embed characters into realistic scenes. For the Noise Background illusions, we first generate images filled with a specific noise texture, and then subtly adjust the local texture attributes within the character regions to embed them. More details of IlluChar are provided in Appendix B.

#### 3.3 Evaluation and Results

We evaluate six representative state-of-the-art MLLMs (Qwen [4], GLM [15], GPT [27], Gemini [9], and Claude [2] models), which are widely deployed MLLMs in real-world applications, and cover both open- and closed-source models with diverse architectures. We additionally recruit 10 human annotators for comparison.

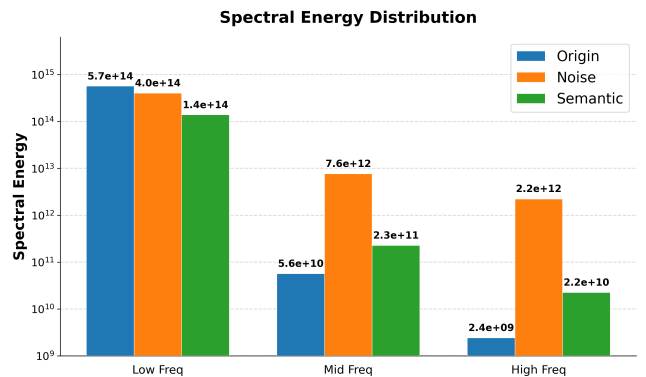


**Figure 3: Spectral energy distribution comparison between original and illusion images.**

Results are presented in Table 1. We report the recognition accuracy on both original and illusion images, along with the performance drop ( $\Delta \downarrow$ ) from original to illusion images. Our observations are as follows:

(1) **All models exhibit vulnerabilities to illusion images.** While human participants consistently achieve near-perfect accuracy, all models suffer substantial performance drops (over 65%) on illusion images of all settings. Besides, we observe that for most models, the accuracies on Semantic Backgrounds are lower than those on Noise Backgrounds, indicating that they are more vulnerable to realistic scenes.

(2) **All models demonstrate limited robustness to the scale variations of hidden characters.** As shown in Table 1, model’s accuracy decreases as the character size gets larger, suggesting that MLLMs lack sufficient robustness to the scale diversity.

### 4 Mechanism: High-Frequency Attention Bias

To better understand the MLLM’s failure, we further investigate its underlying mechanism by examining the distinctive visual characteristics of illusion images and their impact on the model.

#### RQ1: What are special visual features of illusion images?

Compared to the original images, illusion images contain backgrounds with richer visual details, which typically correspond to stronger high-frequency components in the frequency domain. To quantify this feature, we analyze their frequency spectra.

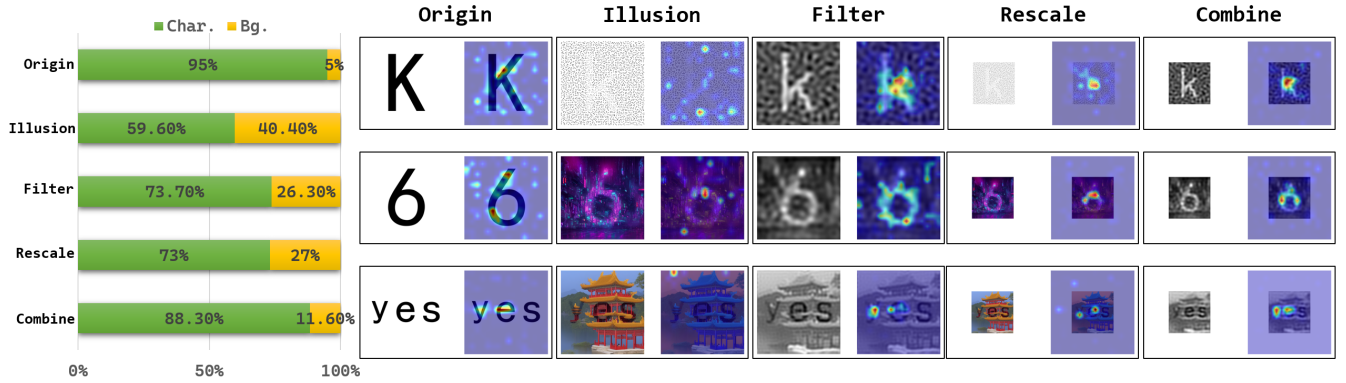


**Figure 4: Analysis of the variance in model’s attention distribution. Left: A quantitative analysis of the model’s high-attention (regions with top 20% attention scores) distribution. Right: Three representative examples.**

Following prior work [31], we adopt **spectral energy distribution** to measure the magnitude of different frequency components of an image. Let  $F(u, v)$  denote the frequency representation of an image  $I \in \mathbb{R}^{H \times W}$ , obtained via Fast Fourier Transform (FFT),

$$F(u, v) = \sum_{x=0}^{H-1} \sum_{y=0}^{W-1} I(x, y) e^{-j2\pi(\frac{ux}{H} + \frac{vy}{W})}, \quad (1)$$

the spectral energy at frequency  $r$  is then defined as

$$E(r) = \sum_{\sqrt{u^2+v^2} \in [r, r+1)} |F(u, v)|^2. \quad (2)$$

For comparison, we aggregate the energy into low- ( $r \leq 100$ ), mid- ( $300 \leq r \leq 400$ ), and high- ( $r \geq 500$ ) frequency bands. As shown in Figure 3, compared to original images, illusion images exhibit significantly higher spectral energy in the middle- and high-frequency bands, regardless of the background types. The result suggests that both types of backgrounds introduce high-frequency signals, while hidden characters are primarily encoded in relatively lower-frequency components.

#### RQ2: How do high-frequency backgrounds affect the model?

To investigate how high-frequency signals influence the model’s behavior, we analyze its attention distribution. Since most MLLMs adopt the CLIP-ViT-based [23] visual encoder [19], we select it as a representative backbone for our analysis to ensure its generalizability across different MLLM architectures. We then employ a Transformer-specific explainability method [6] to obtain attention maps that precisely reflect the model’s internal focus.

Specifically, we measure the proportion of the model’s high-attention regions located within character areas versus background areas to show its variance. As shown in Figure 4, the model assigns nearly all attention to the character areas in original images, while dropping substantially to below 60% on illusion images, showing a significant attention shift toward the background areas. As shown in the three examples, this phenomenon is consistently observed across both background types and different hidden scales, thereby preventing the model from recognizing hidden characters.

Combined with the preceding frequency-domain analysis, it is suggested that the model tends to focus on high-frequency background information rather than the relatively lower-frequency hidden patterns, regardless of the background types or the character scale. We term this distraction as **high-frequency attention bias**.

## 5 Mitigation Method

### 5.1 Inspiration: Human Perceptual Strategies

We observe that the high-frequency attention bias also exists in humans. When encountering illusion images, they are initially drawn to the fine-grained backgrounds as well. However, they can instinctively adopt two perceptual adjustment strategies—**squinting eyes and viewing the image from afar**—to suppress the distracting backgrounds and obtain a clearer perception, thereby refocusing on hidden patterns. Moreover, humans can dynamically adapt these adjustments to illusions of varying hidden scales and backgrounds, further enhancing their ability to perceive more diverse images.

In contrast, current MLLMs lack such perceptual strategies. They can only take the original image as the only input and cannot spontaneously transform it into a clearer one, making them unable to mitigate the high-frequency attention bias.

### 5.2 The Strategy of Multi-Scale Perception

To bridge this perceptual gap between models and humans’ visual capability, we propose **the Strategy of Multi-Scale Perception (SMSP)**, a plug-and-play framework for MLLMs that simulates the human perceptual strategies. SMSP is designed to achieve three primary objectives:

- **Attention Recalibration:** Mitigating the model’s attention bias by introducing a visual perceptual bottleneck to suppress the high-frequency signals.
- **Scale-Diversity Handling:** Consistently improving the model’s recognition performance across hidden patterns of varying spatial scales.
- **Original Capability Preservation:** Ensuring minimal degradation of the model’s foundational visual reasoning capabilities on standard, OOD tasks.

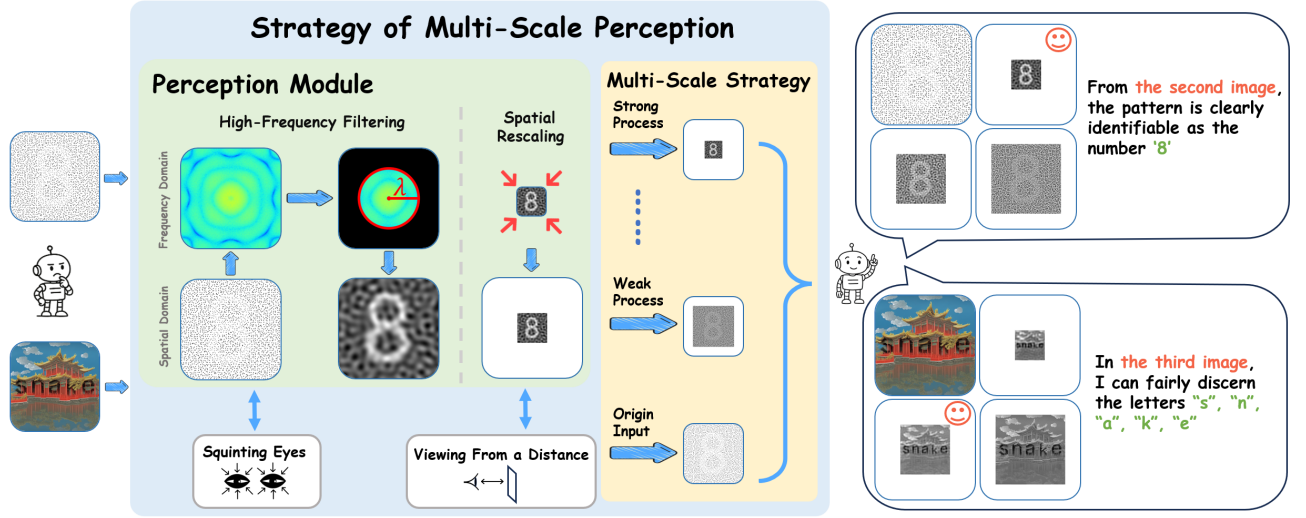


Figure 5: An outline of the Strategy of Multi-scale Perception (SMSP). Two examples are provided to demonstrate the whole process and illustrate how models identify hidden characters with the help of SMSP.

As illustrated in Figure 5, SMSP consists of two key components, **Perception Module** and **Multi-Scale Strategy**, to reach the goals.

**5.2.1 Perception Module.** The Perception Module acts as a high-frequency signal bottleneck. It simulates two human perceptual adaptation strategies—squinting and viewing the image from a distance—to prune high-frequency details, thereby enabling the model to re-allocate its attention toward hidden contents. Specifically, it applies two sequential operations:

- **High-Frequency Filtering:** To simulate human squinting which biologically filters out high-frequency visual noise, we first transform the input illusion image  $I$  into its frequency representation  $F(u, v)$  using Equation 1, and then apply a low-pass filter to discard all the noisy high-frequency signals above a specific frequency threshold  $\lambda$ .
- **Spatial Rescaling:** To simulate human viewing afar, which prioritizes global structure over local textures, we downscale the image with a scale factor  $s$ , and pad it back to its original resolution with a clean white background. This operation further compresses the background information, and makes the hidden content denser and easier for the model to recognize.

Formally, given a perception parameter pair  $(\lambda, s)$ , the Perception Module processes an input illusion image  $I$  into a perception-adjusted variant  $\tilde{I} = \mathcal{P}_{(\lambda, s)}(I)$ , where  $\mathcal{P}$  denotes the Perception Module. The complete processing procedure is outlined in Algorithm 1.

To preliminarily validate its effectiveness, we again trace the variance in the model’s attention distribution. As shown in Figure 4, applying either High-Frequency Filtering or Spatial Rescaling operation can effectively make the image clearer and restore the model’s focus. Furthermore, their combination yields a synergistic effect, achieving the best recovery from 59.6% to 88.3%. This demonstrates that the Perception Module can effectively mitigate

**Algorithm 1:** Image processing procedure in the Perception Module

---

**Input:** Input image  $I \in \mathbb{R}^{H \times W}$ , filtering threshold  $\lambda \in (0, 1)$ , rescaling factor  $s \in (0, 1)$

**Output:** Processed image  $\tilde{I}$

```

/* Operation 1: High-Frequency Filtering */
1  $F = \text{FFTShift}(\text{FFT2D}(I))$  // Transform the image into frequency domain
2 for  $(u, v)$  in  $(0, H) \times (0, W)$  do
3    $F_{\text{filtered}}[u, v] = \begin{cases} F[u, v], & \sqrt{u^2 + v^2} \leq \min(H, W) \cdot \lambda \\ 0, & \text{otherwise} \end{cases}$ 
// Discard all the high-frequency signals
4  $I_{\text{filtered}} = |\text{IFFT2D}(\text{IFFTShift}(F_{\text{filtered}}))|$  // Transform back into spatial domain
/* Operation 2: Spatial Rescaling */
5  $I_{\text{scaled}} = \text{Resize}(I_{\text{filtered}}, (H \cdot s, W \cdot s))$  // Downscale the filtered image by the scale factor  $s$ 
6  $\tilde{I} = \text{CreateCanvas}(H, W, \text{white})$ 
7  $\text{PasteAtCenter}(\tilde{I}, I_{\text{scaled}})$  // Create a new white canvas and place the downscaled image at the center
8 return  $\tilde{I}$ 

```

---

the high-frequency attention bias, guiding the model to perceive illusion images as a human would.

**5.2.2 Multi-Scale Strategy.** We further employ the Multi-Scale Strategy to address the scale diversity and preserve the model’s original performance on OOD tasks.

First, the Multi-Scale Strategy generates  $K$  different perceptually processed variants  $\tilde{I}_i$  using the Perception Module, each with a distinct parameter pair  $(\lambda_i, s_i)$ . For the variant with the strongest

**Table 2: Accuracies (%) of six MLLMs with different methods on IlluChar.**

Method	Origin				Noise				Semantic				Origin				Noise				Semantic			
	L	M	S	Avg.	L	M	S	Avg.	L	M	S	Avg.	L	M	S	Avg.	L	M	S	Avg.	L	M	S	Avg.
	<b>Qwen3-VL-8B-Instruct</b>												<b>GLM-4.5V</b>											
Vanilla	87.1	99.3	97.1	93.2	0.6	11.4	48.7	16.7	2.4	6.4	6.7	3.8	93.1	97.1	97.1	95.3	1.3	26.3	75.7	28.5	3.6	6.0	13.3	4.9
CoT	86.6	99.3	97.9	93.2	1.0	12.3	49.9	17.5	1.6	8.9	6.7	3.9	92.2	92.9	96.4	93.6	1.5	24.3	74.7	27.7	3.3	6.7	10.7	4.7
Filtered	94.4	99.3	97.9	96.7	20.9	59.1	17.1	30.3	26.0	81.9	80.0	44.8	94.0	94.3	81.4	90.6	27.3	97.1	51.7	53.1	30.5	90.8	85.3	50.5
Blur with Histogram	90.9	95.0	10.0	69.9	42.6	66.0	1.4	37.7	41.8	42.9	6.7	39.6	90.5	92.9	12.1	69.7	45.4	84.7	6.0	45.4	37.1	64.5	28.0	43.8
<b>SMSP (Ours)</b>	<b>95.3</b>	<b>100.0</b>	<b>97.9</b>	<b>97.3</b>	<b>79.1</b>	<b>95.4</b>	<b>93.0</b>	<b>87.3</b>	<b>74.0</b>	<b>83.7</b>	<b>82.7</b>	<b>77.2</b>	<b>97.8</b>	<b>100.0</b>	<b>98.6</b>	<b>98.6</b>	<b>69.9</b>	<b>97.4</b>	<b>92.1</b>	<b>83.5</b>	<b>58.5</b>	<b>92.9</b>	<b>88.0</b>	<b>69.8</b>
	<b>Qwen3-VL-235B-A22B-Instruct</b>												<b>Claude-Sonnet-4.5</b>											
Vanilla	95.3	100.0	99.3	97.7	0.9	16.4	55.4	20.0	2.7	7.8	6.7	4.4	75.0	97.9	97.9	87.5	1.4	1.7	0.3	1.2	3.0	3.2	9.3	3.5
CoT	94.8	100.0	100.0	97.7	1.7	15.9	52.9	19.6	3.0	6.4	9.3	4.4	75.0	97.9	98.6	87.7	1.5	1.9	0.0	1.2	5.3	3.9	9.3	5.2
Filtered	97.4	100.0	96.4	97.9	24.4	73.1	28.6	38.9	33.9	88.3	93.3	52.7	79.3	97.9	65.7	80.7	6.4	28.0	2.6	11.2	9.1	46.8	49.3	22.0
Blur with Histogram	94.8	99.3	21.4	76.0	42.9	80.0	3.1	42.2	59.5	60.6	17.3	56.8	59.5	57.9	0.7	43.0	25.8	60.0	3.6	29.1	7.0	13.1	0.0	8.2
<b>SMSP (Ours)</b>	<b>99.6</b>	<b>100.0</b>	<b>100.0</b>	<b>99.8</b>	<b>79.7</b>	<b>98.0</b>	<b>94.0</b>	<b>88.6</b>	<b>78.2</b>	<b>89.7</b>	<b>94.7</b>	<b>82.4</b>	<b>86.6</b>	<b>99.3</b>	<b>98.6</b>	<b>93.4</b>	<b>41.3</b>	<b>80.6</b>	<b>65.4</b>	<b>58.6</b>	<b>32.2</b>	<b>61.0</b>	<b>60.0</b>	<b>41.9</b>
	<b>GPT-5.2</b>												<b>Gemini-2.5-Pro</b>											
Vanilla	77.2	99.3	98.6	89.1	3.1	2.9	26.0	9.3	4.0	1.4	4.0	3.3	91.4	98.6	97.1	94.9	1.7	17.1	74.4	25.8	4.7	4.6	12.0	5.2
CoT	77.2	97.9	<b>99.3</b>	88.9	3.3	2.9	26.7	9.6	5.3	1.4	4.0	4.2	92.2	98.6	97.9	95.5	1.2	17.0	68.9	24.0	4.3	8.5	13.3	6.1
Filtered	75.4	96.4	67.9	79.1	13.9	64.6	33.4	33.1	13.8	66.3	<b>85.3</b>	33.0	<b>97.4</b>	<b>100.0</b>	87.9	95.5	26.5	85.6	43.7	47.3	36.1	77.0	74.7	49.8
Blur with Histogram	69.4	59.3	0.7	47.9	33.4	58.7	2.9	32.0	23.1	24.8	5.3	22.3	88.8	98.6	97.9	93.9	45.2	18.9	68.9	44.5	36.2	11.0	13.3	27.8
<b>SMSP (Ours)</b>	<b>87.9</b>	<b>99.3</b>	98.6	<b>93.9</b>	<b>44.8</b>	<b>85.1</b>	<b>70.6</b>	<b>62.9</b>	<b>38.4</b>	<b>72.3</b>	77.3	<b>50.2</b>	92.7	99.3	<b>97.9</b>	<b>95.9</b>	<b>55.9</b>	<b>91.6</b>	<b>85.6</b>	<b>73.8</b>	<b>45.8</b>	<b>78.0</b>	<b>76.0</b>	<b>56.6</b>

processing strength (smallest  $\lambda$  and  $s$ ), it experiences the most aggressive filtering and downscaling, making it effective to reveal large-scale patterns. Conversely, milder variants (larger  $\lambda$  and  $s$ ) are suited for smaller patterns to avoid blurring out hidden contents. We arrange these variants by their processing strength, from strong to weak:

$$\lambda_1 < \lambda_2 < \dots < \lambda_K, \quad s_1 < s_2 < \dots < s_K. \quad (3)$$

Subsequently, inspired by the multi-scale pyramid paradigm in classical image processing [1], we formulate these perception parameters as a geometric progression. By first empirically anchoring the boundary parameters  $(\lambda_1, s_1)$  and  $(\lambda_K, s_K)$ , we then interpolate other parameters geometrically:

$$\lambda_i = \lambda_1 \cdot \left(\frac{\lambda_K}{\lambda_1}\right)^{\frac{i-1}{K-1}}, \quad s_i = s_1 \cdot \left(\frac{s_K}{s_1}\right)^{\frac{i-1}{K-1}}, \quad i = 2, \dots, K-1. \quad (4)$$

We further guarantee the model’s original capabilities by incorporating the original image  $I$  as an additional input, compensating for any original visual details lost during the perceptual operations.

Ultimately, SMSP generates an input tuple with  $K + 1$  images:

$$I_{\text{SMSP}} = (I, \tilde{I}_1, \tilde{I}_2, \dots, \tilde{I}_K), \quad (5)$$

where  $\tilde{I}_i = \mathcal{P}_{(\lambda_i, s_i)}(I)$  denotes the  $i$ -th perceptually adjusted variant. By jointly feeding these images into MLLMs, SMSP enables the model to access and focus on the most informative variant, which aligns with the humans’ ability of dynamically adjusting perception to understand different images.

## 6 Experiments

### 6.1 Settings

*Dataset & Models.* We evaluate the performance of six MLLMs on IlluChar to perform our study. The evaluated models are the same in Section 3.3, including Qwen3-VL-8B-Instruct (235B) [4], GLM-4.5V [15], GPT-5.2 [27], Gemini-2.5-Pro [9], and Claude-Sonnet-4.5 [2].

*Baselines.* Due to the limited number of effective methods for visual illusions, we compare our method against four baselines: (1) **Vanilla**: The original models without any skills. (2) **Chain-of-Thought Prompting (CoT)** [28]: We use CoT prompting technique to guide models to imagine visualizing the image using the proposed perceptual strategies. (3) **Filtered** [25]: a sequence of Gaussian blurs are applied to the image, followed by an additional sharpening operation. (4) **Blur with Histogram** [22]: it first applies a blur operation, and then equalizes the histogram of image luminance.

*Evaluation.* We evaluate the recognition accuracy of MLLMs on both original and illusion character images. We employ a hybrid evaluation method that combines both strict string-matching and GPT-instructed techniques (more details are provided in Appendix C). To assess its reliability, we manually verify the evaluation results on 100 randomly sampled instances. The evaluation method achieves 99% agreement with human judgment, demonstrating its high reliability.

*SMSP Parameter Settings.* To effectively cover various scales of hidden contents, we set the variant number to  $K = 3$ . For perception parameters, we first determine the boundary parameters  $(\lambda_1, s_1)$  and  $(\lambda_K, s_K)$  using small validation subsets, and then derive other parameters via the geometric interpolation in Equation 4. A detailed analysis of the parameter selection is provided in Section 6.3.

### 6.2 Main Results

We report the results in Table 2. Our findings are as follows:

(1) **SMSP consistently improves performance on illusion images across all models and background types.** As shown in Table 2, SMSP substantially boosts accuracies on illusion images for all evaluated models, demonstrating its strong transferability. Moreover, the significant improvements are observed on both Noise and Semantic background illusions, showing its effectiveness across different illusion backgrounds. For example, the average accuracy of Qwen3-VL-8B-Instruct significantly increases from 16.7% and

3.8% to 87.3% and 77.2% on Noise and Semantic backgrounds, respectively. Averaged over all illusion images (Noise + Semantic), its overall accuracy improves from 13.0% to 84.0%, significantly outperforming baseline methods.

(2) **SMSP consistently improves performance across all hidden character scales.** While baseline methods typically achieve improvements on illusions with partial character scales, their gains remain limited on others. In contrast, SMSP consistently improves accuracies across all the scales, demonstrating its effectiveness in handling the scale diversity of hidden characters.

(3) **SMSP preserves—and often enhances—accuracies on original clean inputs.** Unlike baseline methods that often degrade model performance on already high-accuracy original images, SMSP improves illusion accuracy while maintaining and often slightly improving performance on clean inputs, demonstrating its robustness.

### 6.3 Ablation Study

*Effect of SMSP Components.* We perform ablation studies on Qwen3-VL-8B-Instruct to isolate the contributions of each component. Specifically, we examine the following configurations: (1) the complete SMSP framework; (2) **w/o High-Frequency Filtering** and **w/o Spatial Rescaling**, which remove each operation from the Perception Module, respectively; and (3) **Single Processed Variant** ( $i = 1, 2, 3$ ), which retains only one processed variant together with the original image, where  $i$  denotes the selected variant. We report the average accuracy on original images, and scale-wise results averaged on illusion images.

As shown in Table 3, removing either High-Frequency Filtering or Spatial Rescaling leads to a noticeable performance degradation, indicating that the two operations provide complementary benefits and are both indispensable. Moreover, using only a single perceptual variant demonstrates limited performance across all hidden pattern scales. Each performs well only within a narrow range of scales, while failing to generalize to others. The results confirm the necessity of the Multi-Scale Strategy, which can effectively mitigate the limitation of perceiving images with a fixed strength.

**Table 3: Ablation study on Qwen3-VL-8B-Instruct.**

Method	Origin	Illusion		
		Large	Medium	Small
<b>SMSP</b>	97.3	<b>77.2</b>	<b>92.1</b>	<b>92.0</b>
<i>Analysis of the Perception Module</i>				
w/o Low-pass Filtering	96.3	31.8	84.3	87.9
w/o Resizing with Padding	95.5	42.8	88.9	91.2
<i>Analysis of the Multi-Scale Strategy</i>				
Single Processed Variant ( $i = 1$ )	96.1	76.1	65.4	47.0
Single Processed Variant ( $i = 2$ )	<b>98.0</b>	54.3	90.5	74.7
Single Processed Variant ( $i = 3$ )	95.9	15.1	87.2	88.0

*Empirical Analysis of Boundary Parameters.* To determine the optimal boundary parameters ( $\lambda_1, s_1$ ) and ( $\lambda_K, s_K$ ), we utilize a validation set containing hidden characters with extreme scales (i.e., the largest and smallest characters). This allows us to identify the

most effective processing strengths for the strongest and weakest variants, respectively. We conduct a grid search on the validation set to find the best parameters. As shown in Figure 6,  $\lambda_1 = 0.012$  and  $s_1 = 0.1$  yield the best performance on samples with the largest hidden characters, while  $\lambda_K = 0.05$  and  $s_K = 0.4$  perform best on the smallest character samples. Consequently, we leverage these settings for the boundary parameters in all experiments.

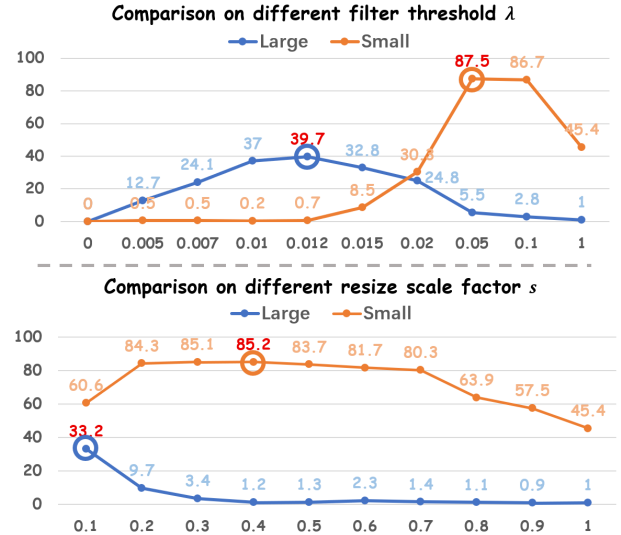


**Figure 6: Empirical selection of SMSP boundary parameters. Accuracies are evaluated on samples with the largest and smallest hidden characters.**

*Discussion on Processed Variant Number  $K$ .* We further analyze the impact of the variant number  $K$  on both recognition accuracy and computational cost. For each  $K$ , the perception parameters are determined using the best boundary parameters and Equation 4. As shown in Figure 7, all tested values of  $K$  consistently and effectively improve performance across various hidden pattern scale ranges (above 75%). The overall accuracy generally increases as  $K$  grows, indicating that additional variants enhance scale coverage. However, when  $K$  becomes excessively large (e.g.,  $K \geq 4$ ), the performance gain becomes marginal, suggesting diminishing returns from further increasing the number of variants.

Furthermore, we quantify the computational cost introduced by SMSP. As shown in Table 4, compared to the vanilla model, SMSP increases the number of input tokens and runtime, both of which grow with the variant number  $K$ . Balancing the performance and the efficiency, we adopt  $K = 3$  as the default setting, which achieves 84.3% accuracy while moderately increasing the runtime from 1.08s to 1.43s (1.32 $\times$ ), showing a favorable trade-off. The results further indicate that despite introducing additional input tokens, SMSP maintains competitive inference efficiency, which aligns with humans' rapidly perceptual adjustments towards illusions, instead of requiring additional knowledge acquiring and training process.

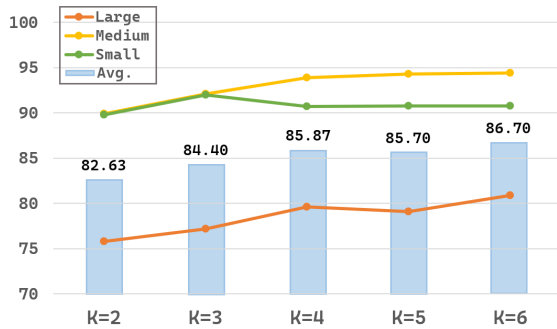


Figure 7: Comparison of the model’s accuracy (%) on illusion images across different hidden pattern scale ranges for varying processed variant numbers  $K$ .

Table 4: Comparison of per-sample computational costs across different variant numbers  $K$  and the vanilla setting.

Cost	Vanilla	K=2	K=3	K=4	K=5	K=6
Input Tokens	1023	1986	2949	3912	4875	5838
Runtimes	1.08	1.30	1.43	1.77	1.92	2.07

## 6.4 Generalization Ability

To assess whether SMSP can generalize beyond character-based illusions, we evaluate its performance on illusions embedding other types of patterns [25], such as animals [18], FashionMNIST [30] and MNIST [17]. Inspired by the HatefullIllusion dataset [22], we also evaluate our methods on detecting illusion images with harmful patterns. As shown in Table 5, SMSP consistently achieves the highest accuracy on illusion images of all hidden pattern types, demonstrating its strong generalization ability.

Table 5: Accuracies (%) of different methods on illusion images with different hidden pattern types.

Method	Animals	Fashion-MNIST	MNIST	Harmful Pattern
Vanilla	34.0	8.5	22.0	4.3
Filtered	93.5	50.5	71.5	66.8
Blur with Histogram	71.0	29.0	76.0	63.5
SMSP	<b>97.5</b>	<b>51.5</b>	<b>88.0</b>	<b>71.0</b>

## 6.5 General Capability Preservation

To ensure that SMSP is safe for general deployment, we evaluate its compatibility on three standard Visual Question Answering (VQA) tasks: SimpleVQA [8], MMStar [7], and RealWorldQA [29]. As reported in Table 6, SMSP maintains the model’s original performance, demonstrating the strategy does not interfere with the model’s original visual reasoning capabilities. To further isolate the source of this robustness, we also evaluate SMSP without the original input branch. The results show a substantial performance drop, indicating that the inclusion of the original image is essential

Table 6: Accuracies (%) of different methods on standard VQA tasks, with the model’s original performances as a reference.

Method	SimpleVQA	MMStar	RealWorldQA
Vanilla	47.5	71.0	70.0
Filtered	14.5	26.5	45.5
Blur with Histogram	9.5	24.0	45.5
SMSP	<b>46.5</b>	<b>68.0</b>	<b>71.0</b>
w/o Original Input	5.0	25.5	44.0

and enough for safeguarding the model’s standard visual reasoning performance.

## 6.6 Case Study

We present two representative examples in Figure 8 to illustrate the effect of SMSP.

In the first example, a large and complex Chinese character is embedded within a realistic scene. For the Filtered and the Blur with Histogram methods, they fail to effectively remove background distractions and preserve the character’s structure, making it difficult for the model to recognize. In contrast, SMSP provides clearer perception-adjusted variants (the second and third images). After considering four input variants, the model can successfully identify

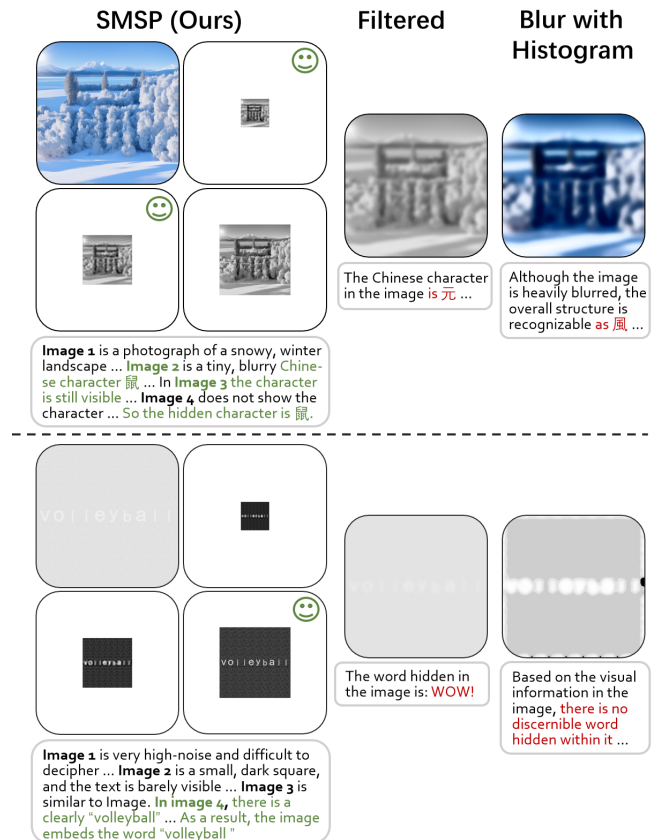


Figure 8: Case study on Qwen3-VL-8B-Instruct.

the character from strongly processed variants. The second example conceals a small English word in a noise texture, and both baseline methods excessively blur the image. This time, SMSP enables the model to correctly identify the word through the weakest processed variant (the fourth image), which clearly reveals the answer.

The examples demonstrate that four images constructed by SMSP are necessary and effective for MLLMs to perceive illusions with different backgrounds and hidden scales. These variants successfully simulate images perceived by humans under their perceptual adjustments, enabling the model to access clearer and more informative visual representations.

## 7 Conclusion

In this work, we systematically investigate MLLM’s vulnerability to hidden-pattern visual illusions. We construct a comprehensive and challenging dataset IlluChar, and further identify a key failure mechanism, high-frequency attention bias, where models are distracted by high-frequency background information and fail to focus on the lower-frequency hidden content. Based on this mechanism, we propose SMSP, a plug-and-play framework to help models perceive illusion images by simulating human perceptual strategies. Experimental results demonstrate that SMSP consistently and significantly improves performance across all evaluated models on illusion images. For example, it boosts the accuracy of Qwen3-VL-8B-Instruct from 13.0% to 84.0% while maintaining its comparable performance on standard VQA benchmarks, indicating SMSP’s enhancement does not degrade models’ foundational visual reasoning capabilities. Our work provides insights into the perceptual gap between humans and multimodal models, suggesting that certain visual failures may stem from models’ visual perceptual deficiencies, rather than its insufficient knowledge or limited model capacity. Furthermore, the success of SMSP indicates that the perceptual gap can be mitigated through training-free methods, instead of costly retraining. We hope our findings inspire future research on perception-aware multimodal modeling to develop more reliable and human-aligned vision-language systems.

## References

- [1] Edward H Adelson, Charles H Anderson, James R Bergen, Peter J Burt, and Joan M Ogden. 1984. Pyramid methods in image processing. *RCA engineer* 29, 6 (1984), 33–41.
- [2] Anthropic. 2025. Introducing Claude Sonnet 4.5. <https://www.anthropic.com/news/claude-sonnet-4-5>
- [3] Tejas Anvekar, Fenil Bardoliya, Pavan K Turaga, Chitta Baral, and Vivek Gupta. 2025. The Perceptual Observatory Characterizing Robustness and Grounding in MLLMs. *arXiv preprint arXiv:2512.15949* (2025).
- [4] Shuai Bai, Yuxuan Cai, Ruizhe Chen, Keqin Chen, Xionghui Chen, Zesen Cheng, Lianghao Deng, Wei Ding, Chang Gao, Chunjiang Ge, Wenbin Ge, Zhifang Guo, Qidong Huang, Jie Huang, Fei Huang, Binyuan Hui, Shutong Jiang, Zhaohai Li, Mingsheng Li, Mei Li, Kaixin Li, Zicheng Lin, Junyang Lin, Xuejing Liu, Jiawei Liu, Chenglong Liu, Yang Liu, Dayiheng Liu, Shixuan Liu, Dunjie Lu, Ruilin Luo, Chenxu Lv, Rui Men, Lingchen Meng, Xuancheng Ren, Xingzhang Ren, Sibao Song, Yuchong Sun, Jun Tang, Jianhong Tu, Jianqiang Wan, Peng Wang, Pengfei Wang, Qiyue Wang, Yuxuan Wang, Tianbao Xie, Yiheng Xu, Haiyang Xu, Jin Xu, Zhibo Yang, Mingkun Yang, Jianxin Yang, An Yang, Bowen Yu, Fei Zhang, Hang Zhang, Xi Zhang, Bo Zheng, Humen Zhong, Jingren Zhou, Fan Zhou, Jing Zhou, Yuanzhi Zhu, and Ke Zhu. 2025. Qwen3-VL Technical Report. *arXiv preprint arXiv:2511.21631* (2025).
- [5] Ryan Burgert, Xiang Li, Abe Leite, Kanchana Ranasinghe, and Michael Ryoo. 2024. Diffusion illusions: Hiding images in plain sight. In *ACM SIGGRAPH 2024 Conference Papers*. 1–11.
- [6] Hila Chefer, Shir Gur, and Lior Wolf. 2021. Generic attention-model explainability for interpreting bi-modal and encoder-decoder transformers. In *Proceedings of the IEEE/CVF international conference on computer vision*. 397–406.
- [7] Lin Chen, Jinsong Li, Xiaoyi Dong, Pan Zhang, Yuhang Zang, Zehui Chen, Haodong Duan, Jiaqi Wang, Yu Qiao, Dahua Lin, et al. 2024. Are we on the right way for evaluating large vision-language models? *Advances in Neural Information Processing Systems* 37 (2024), 27056–27087.
- [8] Xianfu Cheng, Wei Zhang, Shiwei Zhang, Jian Yang, Xiangyuan Guan, Xianjie Wu, Xiang Li, Ge Zhang, Jiaheng Liu, Yuying Mai, et al. 2025. Simplevqa: Multimodal factuality evaluation for multimodal large language models. In *Proceedings of the IEEE/CVF International Conference on Computer Vision*. 4637–4646.
- [9] Gheorghe Comanici, Eric Bieber, Mike Schaekermann, Ice Pasupat, Naveen Sachdeva, Inderjit Dhillon, Marcel Blistein, Ori Ram, Dan Zhang, Evan Rosen, et al. 2025. Gemini 2.5: Pushing the frontier with advanced reasoning, multimodality, long context, and next generation agentic capabilities. *arXiv preprint arXiv:2507.06261* (2025).
- [10] Ziqi Ding, Gelei Deng, Yi Liu, Junchen Ding, Jieshan Chen, Yulei Sui, and Yuekang Li. 2025. IllusionCAPTCHA: A CAPTCHA based on visual illusion. In *Proceedings of the ACM on Web Conference 2025*. 3683–3691.
- [11] Jinyu Fan and Yi Zeng. 2023. Challenging deep learning models with image distortion based on the abutting grating illusion. *Patterns* 4, 3 (2023).
- [12] Daniel Geng, Inbum Park, and Andrew Owens. 2024. Visual anagrams: Generating multi-view optical illusions with diffusion models. In *Proceedings of the IEEE/CVF Conference on Computer Vision and Pattern Recognition*. 24154–24163.
- [13] Tianrui Guan, Fuxiao Liu, Xiyang Wu, Ruiqi Xian, Zongxia Li, Xiaoyu Liu, Xijun Wang, Lichang Chen, Furong Huang, Yaser Yacoob, et al. 2024. Hallusionbench: an advanced diagnostic suite for entangled language hallucination and visual illusion in large vision-language models. In *Proceedings of the IEEE/CVF Conference on Computer Vision and Pattern Recognition*. 14375–14385.
- [14] Elad Hirsch and Ayellet Tal. 2020. Color visual illusions: A statistics-based computational model. *Advances in neural information processing systems* 33 (2020), 9447–9458.
- [15] Wenyi Hong, Wenmeng Yu, Xiaotao Gu, Guo Wang, Guobing Gan, Haomiao Tang, Jiale Cheng, Ji Qi, Junhui Ji, Lihang Pan, et al. 2025. Gm-4.5 v and glm-4.1 v-thinking: Towards versatile multimodal reasoning with scalable reinforcement learning. *arXiv preprint arXiv:2507.01006* (2025).
- [16] Edward J Hu, Yelong Shen, Phillip Wallis, Zeyuan Allen-Zhu, Yuanzhi Li, Shean Wang, Liang Wang, Weizhu Chen, et al. 2022. Lora: Low-rank adaptation of large language models. *Iclr* 1, 2 (2022), 3.
- [17] Yann LeCun, Léon Bottou, Yoshua Bengio, and Patrick Haffner. 2002. Gradient-based learning applied to document recognition. *Proc. IEEE* 86, 11 (2002), 2278–2324.
- [18] Shanchuan Lin, Anran Wang, and Xiao Yang. 2024. Sdxl-lightning: Progressive adversarial diffusion distillation. *arXiv preprint arXiv:2402.13929* (2024).
- [19] Shuai Liu, Weilin Pu, Chongling Xu, Zishuo Huang, Qian Li, Hang Wang, Chenhao Lin, and Chao Shen. 2024. A Comprehensive Survey of Multimodal Large Language Models: Concept, Application and Safety. (2024).
- [20] Dominique Makowski, Zen J Lau, Tam Pham, W Paul Boyce, and SH Annabel Chen. 2021. A parametric framework to generate visual illusions using python. *Perception* 50, 11 (2021), 950–965.
- [21] Artemis Panagopoulou, Coby Melkin, and Chris Callison-Burch. 2024. Evaluating vision-language models on bistable images. In *Proceedings of the Workshop on Cognitive Modeling and Computational Linguistics*. 8–29.
- [22] Yiting Qu, Ziqing Yang, Yihan Ma, Michael Backes, Savvas Zannettou, and Yang Zhang. 2025. Hate in Plain Sight: On the Risks of Moderating AI-Generated Hateful Illusions. In *Proceedings of the IEEE/CVF International Conference on Computer Vision*. 19617–19627.
- [23] Alec Radford, Jong Wook Kim, Chris Hallacy, Aditya Ramesh, Gabriel Goh, Sandhini Agarwal, Girish Sastry, Amanda Askell, Pamela Mishkin, Jack Clark, et al. 2021. Learning transferable visual models from natural language supervision. In *International conference on machine learning*. PmlR, 8748–8763.
- [24] Robin Rombach, Andreas Blattmann, Dominik Lorenz, Patrick Esser, and Björn Ommer. 2022. High-resolution image synthesis with latent diffusion models. In *Proceedings of the IEEE/CVF conference on computer vision and pattern recognition*. 10684–10695.
- [25] Mohammadmostafa Rostamkhani, Baktash Ansari, Hoorieh Sabzevari, Farzan Rahmani, and Sauleh Eetemadi. 2025. Illusory VQA: Benchmarking and enhancing multimodal models on visual Illusions. In *Proceedings of the Computer Vision and Pattern Recognition Conference*. 2995–3004.
- [26] Haz Sameen Shahgir, Khondker Salman Sayeed, Abhik Bhattacharjee, Wasi Uddin Ahmad, Yue Dong, and Rifat Shahriyar. 2024. Illusionvqa: A challenging optical illusion dataset for vision language models. *arXiv preprint arXiv:2403.15952* (2024).
- [27] Aaditya Singh, Adam Fry, Adam Perelman, Adam Tart, Adi Ganesh, Ahmed El-Kishky, Aidan McLaughlin, Aiden Low, AJ Ostrow, Akhila Ananthram, et al. 2025. Openai gpt-5 system card. *arXiv preprint arXiv:2601.03267* (2025).
- [28] Jason Wei, Xuezhi Wang, Dale Schuurmans, Maarten Bosma, Fei Xia, Ed Chi, Quoc V Le, Denny Zhou, et al. 2022. Chain-of-thought prompting elicits reasoning in large language models. *Advances in neural information processing systems* 35 (2022), 24824–24837.

- [29] xAI. 2024. RealworldQA: A Benchmark for Real-World Spatial Understanding. <https://huggingface.co/datasets/xai-org/RealworldQA> Accessed: 2025-04-26.
- [30] Han Xiao, Kashif Rasul, and Roland Vollgraf. 2017. Fashion-mnist: a novel image dataset for benchmarking machine learning algorithms. *arXiv preprint arXiv:1708.07747* (2017).
- [31] Xueyi Ye, Mingcong Sui, Maosheng Zeng, Zhuo Han, and Hao Wang. 2024. Frequency domain characteristics and optimization of image generation for GANs. (2024).
- [32] Lvmin Zhang, Anyi Rao, and Maneesh Agrawala. 2023. Adding conditional control to text-to-image diffusion models. In *Proceedings of the IEEE/CVF international conference on computer vision*. 3836–3847.
- [33] Yichi Zhang, Jiayi Pan, Yuchen Zhou, Rui Pan, and Joyce Chai. 2023. Grounding visual illusions in language: Do vision-language models perceive illusions like humans? *arXiv preprint arXiv:2311.00047* (2023).
- [34] Yiming Zhang, Zicheng Zhang, Xinyi Wei, Xiaohong Liu, Guangtao Zhai, and Xiongkuo Min. 2025. IllusionBench: A Large-scale and Comprehensive Benchmark for Visual Illusion Understanding in Vision-Language Models. *arXiv preprint arXiv:2501.00848* (2025).

## A Pilot Study on Visual Illusion Images with Different Hidden Patterns

We conduct a pilot study to compare the impact of visual illusion images with different hidden patterns on MLLMs. Specifically, we consider several types of hidden patterns. The first group consists of simple patterns, including animals, MNIST digits, and Fashion-MNIST, which are used in the IllusoryVQA [25] dataset. The second group consists of characters, including digits, English letters, and Chinese characters, which are commonly embedded in illusion images shared on social media. Following [22], we also consider visual illusions that hide harmful or sensitive patterns.

For illusion images containing simple and harmful patterns, we adopt images from IllusoryVQA and HatefullIllusion [22] datasets, respectively. For character-based patterns, since limited existing datasets match our requirements, we construct a small set of additional samples by embedding a single large character into similar realistic scenes, ensuring that the data setting remains comparable to other illusion images.

We evaluate three representative MLLMs on these images. As shown in Figure 9, all models achieve significantly lower accuracy on character-based illusions than on images with simple patterns, and the performance is comparable to that with the more complex harmful patterns. In particular, the accuracy on Chinese character illusions is close to 0%. The results suggest that embedding characters into illusion images poses a great challenge for current MLLMs. This observation further motivates us to construct the comprehensive character-based dataset, IlluChar.

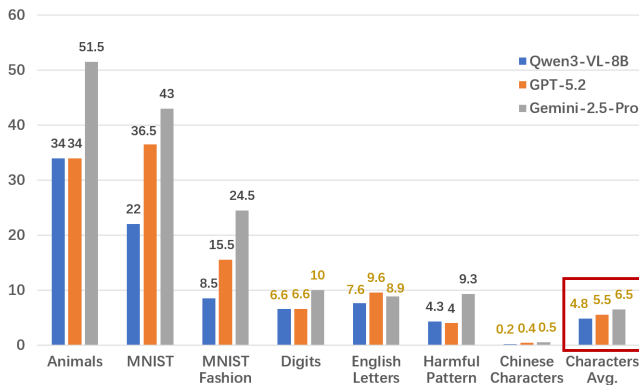


Figure 9: Accuracies (%) on illusion images with different hidden patterns.

## B Dataset Details

### B.1 Details on Dataset Taxonomy

In Section 3.1, we provide a brief overview of the IlluChar dataset. In this section, we present a more detailed description. Based on the type of hidden patterns, IlluChar contains three types of characters:

- **Digits**, including numbers from 0 to 9.
- **English letters**, including uppercase letters A–Z and lowercase letters a–z.

- **Chinese characters**, consisting of 170 commonly used characters. Let  $s$  denote the number of strokes in a character. We incorporate 85 structurally simple characters ( $3 \leq s \leq 9$ ) and 85 structurally complex characters ( $s \geq 13$ ).

Based on the spatial scale of hidden characters, IlluChar can also be categorized into Large, Medium, and Small groups. For each image with a resolution of  $1000 \times 1000$ , suppose the hidden character occupies a region of size  $C_H \times C_W$ . We categorize images according to the following criteria:

- **Large**:  $\max(C_H, C_W) \geq 600$ , where each character occupies a large portion of the image.
- **Medium**:  $200 \leq \max(C_H, C_W) \leq 500$ , where each character occupies a moderate region of the image.
- **Small**:  $\max(C_H, C_W) \leq 150$ , where the character is relatively small but still clearly recognizable.

Based on the background type of illusion images, IlluChar includes two categories: **Semantic Backgrounds** and **Noise Backgrounds**. For Semantic Backgrounds, many prior works [10, 22, 25] have already leveraged this type of background to generate illusions. In our dataset, we further empirically select three thematic realistic scenes as Semantic Backgrounds: *Traditional Chinese Architecture (TC)*, *Cyberpunk City (CC)*, and *Winter Valley (WV)*.

For Noise Backgrounds, we design five types of noise textures: *Vertical Gratings (VG)*, *Gaussian Noise (GN)*, *Halftone Dots (HD)*, *Labyrinth Noise (LN)*, and *Micro-text Noise (MN)*, which are empirically observed to produce strong visual illusion effects.

In Table 7, we present the number of samples in each category.

Table 7: Number of samples in each category.

Categories	Origin	Semantic			Noise				
		TC	CC	WV	VG	GN	HD	LN	MN
<b>Large</b>	232	232	232	232	232	232	232	232	232
<b>Medium</b>	140	98	95	89	140	140	140	140	140
<b>Small</b>	140	28	26	21	140	140	140	140	140

### B.2 Details on Dataset Construction

In this section, we provide a detailed description of the construction process for illusion images.

For illusions with Semantic Backgrounds, we use Stable Diffusion v1.5<sup>1</sup> with a variant of ControlNet<sup>2</sup> to embed characters from the original images (black characters rendered on a white background) into realistic scenes. Empirically, we set the guidance scale to 9 and the number of inference steps to 50 to obtain high-quality illusion images.

For Noise Background illusions with a noise texture  $T \in \{VG, GN, HD, LN, MN\}$ , we generate the image by using the texture with slightly different parameters for the character region ( $p_c$ ) and the background region ( $p_b$ ). This design introduces subtle differences between the character and background regions, thereby producing

<sup>1</sup>The download link to the model: <https://huggingface.co/stable-diffusion-v1-5/stable-diffusion-v1-5>

<sup>2</sup>The download link to the model: [https://huggingface.co/monster-labs/control\\_v1p\\_sd15\\_qrcode\\_monster](https://huggingface.co/monster-labs/control_v1p_sd15_qrcode_monster)

high-quality illusion images. Specifically, an illusion image  $I_{\text{illusion}}$  with character region  $\mathcal{D}_{\text{char}}$  is generated by

$$I_{\text{illusion}}(x, y) = \begin{cases} T_{p_c}(x, y) & \text{if } (x, y) \in \mathcal{D}_{\text{char}} \\ T_{p_b}(x, y) & \text{otherwise.} \end{cases} \quad (6)$$

We further provide the description of each noise texture  $T$ :

- **Vertical Gratings (VG):** a texture composed of black-and-white vertical stripes.  $T_{p_c}$  and  $T_{p_b}$  differ from the width of stripes.
- **Gaussian Noise (GN):** a texture using Gaussian noise.  $T_{p_c}$  and  $T_{p_b}$  differ from the base gray level used for Gaussian noise.
- **Halftone Dots (HD):** a texture composed of randomly distributed dots.  $T_{p_c}$  and  $T_{p_b}$  differ from the size of dots.
- **Labyrinth Noise (LN):** a maze-like binary texture generated by smoothing random noise and applying thresholding.  $T_{p_c}$  and  $T_{p_b}$  differ from the noise distribution.
- **Micro-text Noise (MN):** a texture composed of randomly distributed micro symbols.  $T_{p_c}$  uses '@' and '&' symbols, while  $T_{p_b}$  uses '\$', '%', and '#' symbols.

In Figure 10, we provide illusion images with different backgrounds by embedding the digit '5' as an example.

After the construction, we further perform manual filtering to remove images with unsatisfactory illusion effects, and retain only high-quality samples in IlluChar.

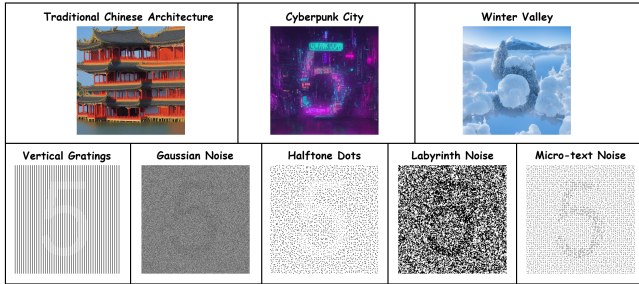


Figure 10: Examples of illusions with different backgrounds.

### B.3 Verification on the Effectiveness of Different Backgrounds

We further verify the effectiveness of embedding characters into the proposed backgrounds. Specifically, we randomly select 100 hidden characters, and compare model performance on their original images and corresponding illusion images.

As shown in Table 8, all types of backgrounds substantially degrade model performance, with accuracies dropping below 10% in all cases. This result demonstrates the effectiveness of all proposed backgrounds in generating challenging illusion images.

## C Evaluation Details

Our evaluation method combines strict string matching and GPT-based evaluation. Given a model response  $y^*$  and the ground-truth answer  $y$ , we consider the following cases:

Table 8: Accuracies (%) of six MLLMs on illusion images with different backgrounds.

Models	Origin	Semantic			Noise				
		TC	CC	WV	VG	GN	HD	LN	MN
Qwen3-VL-8B	86.0	1.0	1.0	5.0	3.0	3.0	0.0	6.0	3.0
GLM-4.5V	95.0	0.0	1.0	6.0	7.0	6.0	3.0	3.0	8.0
Qwen3-VL-235B-A22B	96.0	0.0	1.0	8.0	4.0	6.0	1.0	4.0	4.0
GPT-5.2	81.0	2.0	1.0	9.0	6.0	2.0	1.0	2.0	8.0
Gemini-2.5-Pro	93.0	2.0	4.0	7.0	5.0	5.0	5.0	8.0	9.0
Claude-Sonnet-4.5	85.0	0.0	0.0	9.0	0.0	2.0	1.0	0.0	1.0
<b>Human</b>	-	<b>99.0</b>	<b>100.0</b>	<b>100.0</b>	<b>100.0</b>	<b>98.0</b>	<b>99.0</b>	<b>98.0</b>	<b>100.0</b>

- If  $y \notin y^*$ , the response does not contain the target character. We regard the response as incorrect.
- If  $y \in y^*$ ,  $|y| \geq 3$ , and  $y$  is not a common string that may naturally appear in model responses, we regard the response as correct.
- In all other cases, we employ GPT-4o as an evaluator to determine whether the response is correct.

To validate the reliability of this evaluation method, we randomly sample 100 instances for manual annotation. The agreement between our method and human judgment reaches 99%, indicating that the method is reliable. We provide the prompt template for GPT-based evaluation here:

```

You are a strict evaluator. Your task is to determine whether the model's response correctly identifies the hidden number(s), letter (s), word(s), or Chinese character(s) in the image.

You will be given a ground truth answer, which is the correct hidden content, and a model response, which is the content identified by a specific model. You should compare the model response with the ground truth answer and decide if the model's identification is correct.
- [Correct]: If the model response exactly matches the ground truth answer.
- [Incorrect]: If the model response does not match the ground truth answer.
Your output should only contain your evaluation result, either "Correct" or "Incorrect".

# Example 1
Ground Truth Answer: 5
Model Response: Looking at the image carefully, I can identify the hidden number: 5.
Evaluation: Correct
# Example 2
Ground Truth Answer: animal
Model Response: The hidden word in the image is "ANIMAL".
Evaluation: Correct
# Example 3
Ground Truth Answer: A
Model Response: The hidden letter in the image is B.
Evaluation: Incorrect
# Example 4
Ground Truth Answer: 我
Model Response: The hidden Chinese character in the image is 我.
Evaluation: Correct
# Example 5
Ground Truth Answer: 你好吗
Model Response: The hidden Chinese characters in the image are 我好嘛.
Evaluation: Incorrect

Now it's your turn to evaluate.

Ground Truth Answer: [GROUND_TRUTH]
Model Response: [RESPONSE]
Evaluation:

```

## D Prompts for the Experiments

We provide prompt templates used in Section 6. For Vanilla, Filtered, and Blur with Histogram methods, there is only one image input for the models. They utilize a same default prompt template:

There is a [hidden\_type] in the image, what is it ?

For Chain-of-Thought Prompting (CoT) method, we prompt the models to imagine visualizing the image using the proposed perceptual strategies—squinting eyes and viewing afar. The CoT prompt template is as follows:

You are an expert in solving visual puzzles and optical illusions. Your task is to identify the hidden [hidden\_type] embedded in the image.

The image is designed as an optical illusion, where the character is subtly integrated into the semantic background or noise patterns.

To identify the hidden content, you can simulate human visual behaviors:

1. Imagine squinting your eyes or slightly blurring your vision. Ignore the sharp, high frequency details, textures and noise in the image.
2. Imagine viewing the image from a long distance. You can resize the image smaller in your mind to get a global view of the image. You can combine the two strategies to enhance your perception of the hidden character.

Now, please analyze the image carefully, and identify the hidden [hidden\_type].

For SMSP, each sample is processed into four input images for the model. We provide the model with a brief description of the relationships among these images and prompt it to reason by jointly considering all four images. The prompt template is as followed:

I provide four views of the SAME image, the original view and the global views. There is a SAME [hidden\_type] embedded in these images, with the help of the views, what is it ?

## E Additional Results on MLLMs of Different Sizes

In Section 6, we evaluate SMSP on MLLMs from different families. The results demonstrate its transferability across diverse model architectures. Furthermore, we investigate SMSP’s scalability by testing models of varying sizes from the Qwen3-VL series [4]. Specifically, our evaluation includes models with 2B, 4B, 8B, 30B-A3B, and 235B-A22B parameters, covering a wide range of model scales.

As shown in Table 9, SMSP consistently outperforms baseline methods across all evaluated models, substantially improving their performance on all types of illusion images. These results further demonstrate the effectiveness and robustness of SMSP across models of different scales.

## F Case Study

Apart from the two cases presented in Section 6.6, we provide additional examples here to further illustrate the effectiveness of SMSP. As shown in Figure 11, across various types of illusion images—including variations in hidden character type, character size, and background type—SMSP consistently generates clearer perception-adjusted variants. The model is then able to identify more informative images among them and successfully recognize the hidden content.

**Table 9: Accuracies (%) of Qwen-series models with different methods on IlluChar.**

Method	Origin				Noise				Semantic			
	L	M	S	Avg.	L	M	S	Avg.	L	M	S	Avg.
<b>Qwen3-VL-2B-Instruct</b>												
Vanilla	67.2	97.9	96.4	83.6	0.5	14.6	48.4	17.5	1.3	8.9	2.7	3.4
CoT	67.2	95.0	<b>98.6</b>	83.4	0.7	16.1	44.3	16.8	1.0	11.3	4.0	4.0
Filtered	84.5	<b>99.3</b>	83.6	88.3	6.5	23.7	9.7	12.1	25.9	78.7	<b>80.0</b>	43.9
Blur with Histogram	80.2	88.6	25.0	67.4	33.6	55.9	2.3	31.1	32.9	46.1	14.7	35.1
<b>SMSP (Ours)</b>	<b>88.8</b>	98.6	97.1	<b>93.8</b>	<b>64.8</b>	<b>92.3</b>	<b>86.3</b>	<b>78.2</b>	<b>61.8</b>	<b>90.8</b>	70.7	<b>70.2</b>
<b>Qwen3-VL-4B-Instruct</b>												
Vanilla	75.0	99.3	<b>99.3</b>	88.3	1.0	8.7	45.7	15.4	2.3	7.4	8.0	4.1
CoT	74.1	<b>100.0</b>	98.6	87.9	1.5	8.0	43.7	14.8	2.4	7.8	6.7	4.2
Filtered	88.8	<b>100.0</b>	85.0	90.8	12.2	28.9	12.6	16.9	28.9	75.9	<b>80.0</b>	45.1
Blur with Histogram	89.2	95.0	23.6	72.9	39.5	61.6	1.9	35.2	43.1	48.6	13.3	42.5
<b>SMSP (Ours)</b>	<b>96.6</b>	99.3	97.9	<b>97.7</b>	<b>70.9</b>	<b>92.6</b>	<b>86.9</b>	<b>81.2</b>	<b>65.1</b>	<b>77.0</b>	78.7	<b>69.2</b>
<b>Qwen3-VL-8B-Instruct</b>												
Vanilla	87.1	99.3	97.1	93.2	0.6	11.4	48.7	16.7	2.4	6.4	6.7	3.8
CoT	86.6	99.3	97.9	93.2	1.0	12.3	49.9	17.5	1.6	8.9	6.7	3.9
Filtered	94.4	99.3	97.9	96.7	20.9	59.1	17.1	30.3	26.0	81.9	80.0	44.8
Blur with Histogram	90.9	95.0	10.0	69.9	42.6	66.0	1.4	37.7	41.8	42.9	6.7	39.6
<b>SMSP (Ours)</b>	<b>95.3</b>	<b>100.0</b>	<b>97.9</b>	<b>97.3</b>	<b>79.1</b>	<b>95.4</b>	<b>93.0</b>	<b>87.3</b>	<b>74.0</b>	<b>83.7</b>	<b>82.7</b>	<b>77.2</b>
<b>Qwen3-VL-30B-A3B-Instruct</b>												
Vanilla	93.1	99.3	97.9	96.1	1.4	34.1	62.4	27.0	2.0	3.2	2.7	2.4
CoT	92.2	99.3	97.1	95.5	1.8	31.3	61.1	26.1	2.7	5.7	4.0	3.6
Filtered	93.5	100.0	90.0	94.3	22.5	40.6	17.6	26.1	21.0	85.1	88.0	42.9
Blur with Histogram	92.2	95.7	37.1	78.1	37.4	61.6	2.0	34.3	43.1	56.4	13.3	44.5
<b>SMSP (Ours)</b>	<b>95.7</b>	<b>100.0</b>	<b>100.0</b>	<b>98.0</b>	<b>71.3</b>	<b>95.3</b>	<b>89.6</b>	<b>82.9</b>	<b>64.5</b>	<b>92.2</b>	<b>89.3</b>	<b>73.7</b>
<b>Qwen3-VL-235B-A22B-Instruct</b>												
Vanilla	95.3	100.0	99.3	97.7	0.9	16.4	55.4	20.0	2.7	7.8	6.7	4.4
CoT	94.8	100.0	100.0	97.7	1.7	15.9	52.9	19.6	3.0	6.4	9.3	4.4
Filtered	97.4	100.0	96.4	97.9	24.4	73.1	28.6	38.9	33.9	88.3	93.3	52.7
Blur with Histogram	94.8	99.3	21.4	76.0	42.9	80.0	3.1	42.2	59.5	60.6	17.3	56.8
<b>SMSP (Ours)</b>	<b>99.6</b>	<b>100.0</b>	<b>100.0</b>	<b>99.8</b>	<b>79.7</b>	<b>98.0</b>	<b>94.0</b>	<b>88.6</b>	<b>78.2</b>	<b>89.7</b>	<b>94.7</b>	<b>82.4</b>

In Figure 12, we further present examples of illusions with more diverse hidden patterns selected from the IllusoryVQA [25] dataset. The results further demonstrate the effectiveness of SMSP and highlight its generalizability across a variety of illusion images.

## G Limitations in Fine-tuning Strategy

We further explore model fine-tuning as a potential mitigation strategy. Following [25], we fine-tune Qwen3-VL-4B-Instruct using similar hyperparameters (the parameters are provided in Table 10). We use 2.5k illusion images from IlluChar for training and reserve the remaining data (approximately 1.1k) as the test set. We evaluate the fine-tuned model on both the IlluChar test set and illusion images with other hidden patterns. We then compare it with the vanilla 4B model and the vanilla model enhanced with SMSP.

**Table 10: Hyperparameters used for fine-tuning.**

Hyperparameter		Value
Learning Rate		$1e-5$
Batch Size (per device)		8
Epochs		2
Optimizer		AdamW
Lora [16]	r	64
	lora_alpha	16
	target_modules	all-linear
	dropout	0

As shown in Table 11, the model fine-tuned on IlluChar indeed achieves improved performance on IlluChar itself, but still lags behind SMSP. Furthermore, on illusion images with other hidden patterns, the fine-tuned model performs similarly to the vanilla

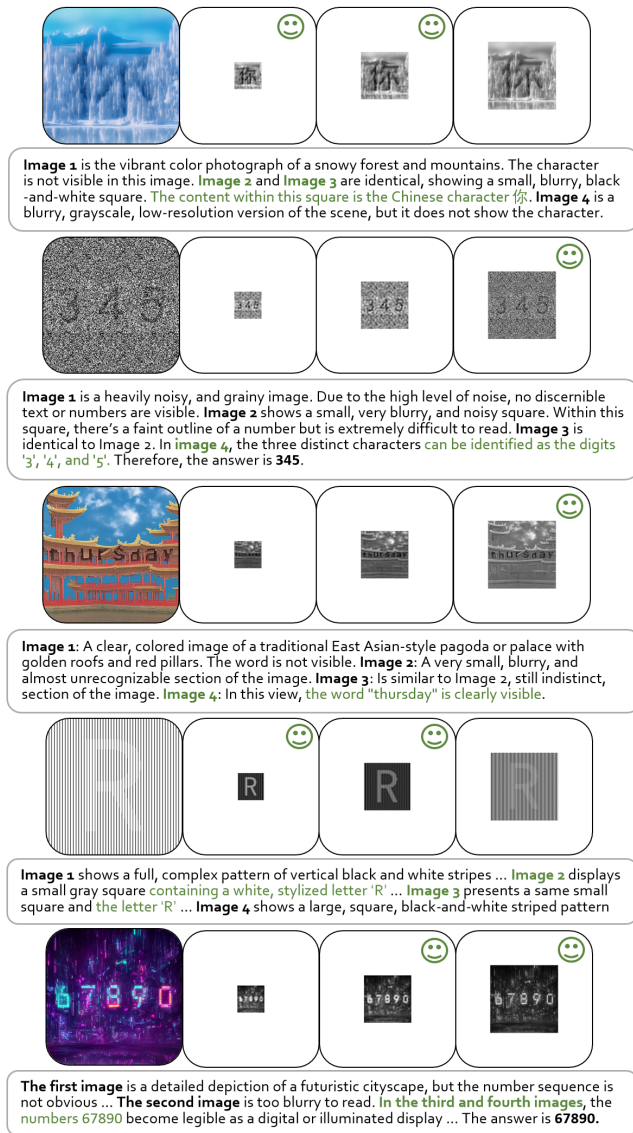


Figure 11: Examples of SMSP on illusions with more diverse settings.

model, suggesting its limited generalization. These results indicate that perception-based improvements cannot be reliably obtained through additional model training alone, highlighting the necessity of explicitly incorporating perceptual strategies.

## H Broader Impact

Our work introduces a novel perception-inspired paradigm for improving the MLLM’s understanding of images by simulating human perceptual strategies. Compared with methods that rely on retraining the original model, our method is simple and training-free, requiring no additional training data and enabling plug-and-play deployment.

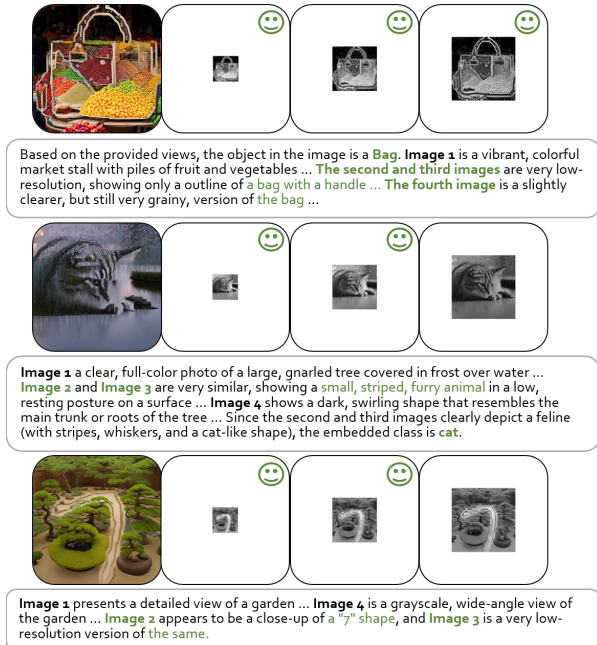


Figure 12: Examples of SMSP on samples in IllusoryVQA [25].

Table 11: Accuracies (%) of the vanilla 4B model, the fine-tuned model, and the SMSP method.

Method	IlluChar	Animals	Fashion-MNIST	MNIST	Harmful Pattern
Vanilla	11.6	33.5	8.5	17.5	1.0
Fine-tuning	22.9	31.5	12.0	19.0	1.5
SMSP	77.9	92.5	48.0	90.5	25.0

Beyond visual illusions, this paradigm may also inspire new perception-driven strategies for more complex tasks, including fine-grained image analysis and video understanding, which enables its broader applications across diverse visual understanding tasks.

## I Limitations and Future Work

Although SMSP significantly improves model performance on illusion images across all evaluated settings, it relies on predefined perceptual parameters and lacks the ability to dynamically adapt to different input images. In addition, the use of fixed parameters increases the number of input images by a factor of four. Although Section 6.3 shows that the resulting time overhead is minimal, it still incurs additional token costs. Future work could investigate training lightweight networks to predict optimal perceptual parameters or dynamically select the most suitable perceptually adjusted variant for each input image.

In addition, as discussed, our work only explores aligning the model’s perceptual strategy with human perception in the context of visual illusions. Future work could build upon the perceptual paradigm introduced by SMSP to design additional visual perception strategies for MLLMs, enabling them to better handle a broader range of tasks.